Journal of Materials and Environmental Science
ISSN : 2028-2508
CODEN : JMESCN

J. Mater. Environ. Sci., 2024, Volume 15, Issue 12, Page 1825-1837

http://www.jmaterenvironsci.com

Modeling of the conditions for preparation of Activated Carbons from *Blighia sapida* (Sapindaceae) shells

Tra B. T. D., Soro Y. *, Briton B.G.H.

Laboratoire des Procédés Industriels de Synthèse, de l'Environnement et des Energies Nouvelles (LAPISEN), Institut National Polytechnique Félix HOUPHOUËT-BOIGNY de Yamoussoukro, BP 1093 Yamoussoukro, Côte d'Ivoire

**Corresponding author*: E-mail : *yaya.soro@inphb.ci*

Received *01 Dec 2024,*
Revised *25 Dec 2024,*
Accepted *26 Dec 2024*

Citation*: Tra B. T. D., Soro Y., Briton B.G.H. (2024) Optimization of the conditions for preparation of Activated Carbons from Blighia sapida (Sapindaceae) shells, J. Mater. Environ. Sci., 15(12), 1825-1837.*

Abstract: The conditions for preparing activated carbons from *Blighia sapida* shells with good adsorption capacities were modeled by a complete factorial plan. Particle size, activating agent, impregnation ratio and activating agent concentration were the factors that influence adsorption capacity of activated carbons. The best experimental conditions were obtained with a particle size of crushed shells of 100 µm, an impregnation ratio of 1/3 and the use of phosphoric acid (H_3PO_4) as an activating agent at a concentration of 30 %. These conditions resulted in a microporous activated carbons with an adsorption capacity of 685.35 mg/g, a total pore volume of 0.905 $cm^3.g^{-1}$, a mean pore diameter of 5.3 nm and a specific surface of 681.12 m^2/g. The determination of the surface functions revealed that activated carbons obtained have an acid character due mainly to lactone, carboxylic acid and phenol functions.

Keywords: *Activated carbon, Chemical activation, Experimental plan, Modeling, Characterization*

1. Introduction

The sharp increase in the world's population associated with high agricultural production generate large quantities of agricultural waste, the recovery of which is at the center of global policies (Basta *et al.*, 2011). Thus, agricultural waste has been recovered in several areas such as energy, biofertilizers, animal feed as well as water depollution (Ouattara *et al.*, 2021). Among the many ways of recovering agricultural waste, the development of activated carbons has aroused great interest because their preparation is economically interesting and their applications in depollution of water contaminated by mining and textile industries, has given good results (Muhammad *et al.*, 2022; Gouré Bi *et al.*, 2021a; Benallou Benzekri *et al.*, 2018; Jodeh *et al.*, 2014).

Activated carbons can be obtained by physical or chemical activation of precursors containing a high carbon content and a low percentage of inorganic matter (Basta *et al.*, 2011). Thus, various activated carbons have been obtained from agricultural waste such as cherry kernel (Jaramillo *et al.*, 2009), olive (Benallou Benzekri *et al.*, 2018), rice husk (Sahu *et al.*, 2009), bean husk (Cabal *et al.*, 2009), rice straw (Basta *et al.*, 2011; Fierro *et al.*, 2010), coconut husk (Atheba *et al., 2014*), coffee shells (Kokora *et al.*, 2018), peanut shells and cocoa pods (Kouadio *et al.*, 2019), plantain spikes (Briton *et al.*, 2020) as well as mango kernel shells (Gouré Bi *et al.*, 2021b). The effectiveness of an

activated carbon is closely linked to its specific surface, which is correlated to the iodine index (Mohammad *et al.*, 2007; Afrane and Achaw, 2008, Nko'o Abuiboto *et al.*, 2016) and optimization of its production process has been reported in literature (Tchakala *et al.*, 2012).

Continuing the recovery of agricultural waste, we focused on the production of activated carbon from shells of *Blighia sapida* (Sapindaceae), known as fisanier. Indeed, this plant is widespread in West African countries and its aril is widely consumed due to its richness in lipids, proteins, vitamins C and mineral elements (Outtara *et al.*, 2011). Its importance comes also from its nutritional, ethnobotanical and cultural potentialities as well as its medicinal and aesthetic values (Ndiaye *et al.*, 2023). Thus, many *Blighia sapida* shells wastes, which represent approximately 63.56 % of the weight of the fruit, are produced each year without appropriate recovery, which leads to environmental pollution.

The present study aims to valorize *Blighia sapida* shells into activated carbons and to model the process of their preparation by acting on the impregnation and carbonization parameters and by following the evolution of iodine index.

2. Materials and methods

2.1. plant material

The fruits of *Blighia sapida* (**Figure 1a**) were collected in December 2022 at the beginning of the dry season in Yamoussoukro (6047'18.762" N and 5015'25.9992" W) in the center of Côte d'Ivoire and identified by Mr. Antoine Amani N'GUESSAN, botanist at the Institut National Polytechnique Félix HOUPHOUËT-BOIGNY (INP-HB) in Yamoussoukro. The fruits were washed, and the shells were isolated then dried at room temperature (25±3°C) for one week and then in an oven at 60°C for 1 hour. The dry shells (**Figure 1b**) were kept in the laboratory until their use to prepare activated carbons (ACs).

a) b)

Figure 1. *Blighia sapida* fruits (a) and dry shells (b)

2.2. Methods

2.2.1. Preparation of activated carbons

Crushed plant material was sieved to give ground materials of size 100 µm and 400 µm, then activated carbons were prepared according to the method used by Gouré Bi et al. (Gouré Bi *et al.*, 2021b) with a slight change in oven temperature (400 °C) and carbonization time (1 hour).

2.2.2. Characterization of activated carbons obtained

2.2.2.1. Determination of iodine value

Iodine value was determined according to the method described by Maazou et al. (Maazou *et al.*, 2018). To 0.05 g of activated carbon in a 100 mL beaker were added 20 mL of a 0.1 N iodine solution. The resulting mixture was stirred for 5 min then filtered. A volume of 10 mL of filtrate was withdrawn from an Erlenmeyer flask and then titrated with 0.1 N sodium thiosulfate solution until the solution is completely discolored. Starch paste was used as a color indicator. The iodine value (mg/g) was determined from **Eqn. 1**.

$$\text{Iodine Value (mg/g)} = \frac{M_{iodine}}{2}\left(\frac{N_i - N_e}{m}\right)V \qquad \textbf{Eqn. 1}$$

Where N_i and N_e were initial normality of iodine solution and normality of iodine solution after filtration, m (g), V (mL) and M_{iodine} represented mass of activated carbon, volume of iodine solution at 0.2 N and molar mass of iodine, respectively.

2.2.2.2. Determination of dry matter, moisture and ash contents

Dry matter, moisture and ash contents were determined according to the method described by Kokora et al. (Kokora *et al.*, 2018).

2.2.2.3. Determination of methylene blue index

Methylene blue index was determined according to the method described by Briton et al. (Briton *et al.*, 2020).

2.2.2.4. Determination of hydrogen potential at the point of zero charge

The method described by Crini (Crini, 2006) was used for determination of hydrogen potential at zero charge point (pHpzc).

2.2.2.5. Determination of surface functional groups

The surface functional groups (acids and bases) of activated carbon were determined according to the method described by Boehm (Seung Kim and Rae Park, 2016). The functional groups on the surface of the AC were identified using Fourier Transform Infrared Spectrometry (FTIR). Thus, carbon powder pellets were produced by mixing 100 mg of KBr and 1 mg of finely ground activated carbon serving as a reference in a range of wave numbers between 4 000 and 650 cm^{-1} with a resolution of 1 cm^{-1} using an ALPHA BRUCKER type spectrometer. Then, the electric field induced by the incident electromagnetic wave may interfere with the dipole moment of molecules present in the sample to be analyzed. Finally, responses obtained were collected in the form of IR spectra with characteristic bands of functional groups present on the surface of AC.

2.2.2.6. Scanning Electron Microscopy

Scanning Electron Microscopy (SEM) was undertaken to determine the morphological characteristics of ACs. The analysis was performed on a Hirox SH 4000 M model device combined with energy dispersive X-rays.

2.2.2.7. Elemental composition

Energy Dispersion Spectrometry (EDS) was used to determine the elemental composition of activated carbon. The test was carried out with 100 mg of adsorbent.

2.2.2.8. X-ray Diffraction

X-Ray Diffraction (XRD) was used to know the structure of activated carbon. The XRD apparatus used in this study is the diffractometer Rigaku Ultima IV. During analyses, monochromatic copper radiation Kα (λ = 1.5406 Å, 40 kV, 40 mA) was used and applied at a scanning rate of 0.01° min^{-1} and an angle 2θ between 0 and 70.

2. 2.2.9. Determination of specific surface and porosity

The nitrogen (N_2) adsorption-desorption method was used to determine the specific surface and pore volume. The specific surface of activated carbon was calculated by the Brunauer, Emmett and Teller (BET) method (Gouré Bi *et al.*, 2021b).

2.2.3. Experimental plan for preparation of activated carbon of *Blighia sapida* shells

2.2.3.1. Choice of factors

Particle size (X_1), activating agent (X_2), impregnation ratio (X_3) and activating agent concentration (X_4) were considered as impregnation input factors and iodine value (Y) was considered as response. The choice of these factors was justified by the importance of their influence on the adsorbent power during preparation of an activated carbon (Gueye *et al.*, 2014). The range of values of the selected factors, according to the complete factorial plan, is presented in **Table 1**.

Table 1. Values of selected factors

Coding	Factors	Value (-1)	Value (+1)
X_1	Particle size (µm)	100	400
X_2	Activating agent	NaOH	H_3PO_4
X_3	Impregnation ratio (m/m)	1/1	1/3
X_4	Activating agent concentration (%)	10	30

A mass (m) of ground *Blighia sapida* shells of sizes of 100 µm or 400 µm and a volume (v) of orthophosphoric or sodium hydroxide solution (at 10 % or 30 %) in ratios (m/m) 1/1 or 1/3 were introduced into a 250 mL beaker. The mixtures were stirred for 24 h on a magnetic stirrer at room temperature. After impregnation, the samples were removed and then dried in an oven for 24 hours at 105°C so that all the solvent (water) evaporated before carbonization.

2.2.3.2. Modeling

The complete two-level factorial plan with k factors was used to reduce the number of experiments to be performed without compromising the quality of desired results, to understand the influence of each factor and the interactions between them, and finally to model the conditions of the process (Adjoumani *et al.*, 2019; Eddebbagh *et al.*, 2016; Brasil *et al.*, 2005).

The iodine index was chosen as a response to evaluate the development of microporosity through the iodine adsorption capacity of activated carbons prepared during the tests. It is a good indicator for evaluating the quality of prepared activated carbons. For this purpose, the postulated mathematical model linking response to different factors is a first order equation (**Eqn. 2**).

$$Y = b_0 + b_1X_1 + b_2X_2 + b_3X_3 + b_4X_4 + b_{12}X_1X_2 + b_{13}X_1X_3 + b_{14}X_1X_4 + b_{23}X_2X_3 + b_{24}X_2X_4 + b_{34}X_3X_4 \quad \textbf{Eqn. 2}$$

where Y is the response (iodine value). X_1, X_2, X_3 and X_4 are the coded variables for particle size, activating agent, impregnation ratio and activating agent concentration, respectively. b_0 is a

constant, b_1, b_2, b_3 and b_4 represent the weight of particle size, activating agent, impregnation ratio and activating agent concentration, respectively. b_{12}, b_{13}, b_{14}, b_{23}, b_{24} and b_{34} represent the effects of interaction between particle size and activating agent, between particle size and impregnation ratio, between particle size and activating agent concentration, between activating agent and impregnation ratio, between activating agent and its concentration and between impregnation ratio and activating agent concentration, respectively.

The statistical analysis of the experimental results was carried out with the Nemrodw software (New efficient methodology for research using optimal design, LPRAI - Marseille, France) version 2000. The coefficients and their significance were determined by statistical analysis, considering that a coefficient is statistically significant if its absolute value is greater than twice the standard deviation (2σ) (Assidjo *et al.*, 2005). All tests were carried out in triplicate and the results are generally expressed as: value ± standard deviation.

3. Results and discussion

3.1. Modeling of the conditions for preparing activated carbon

3.1.1. Statistical analysis and model equation

Tables 2 show the results of the experimental plan.

Table 2. Results of the experimental plan

Tests	Particle Size (µm) (X_1)	Activation agent (X_2)	Impregnation ratio (g/g) (X_3)	Activating agent concentration (%) (X_4)	Iodine index (mg/g) (Y)
1	100	NaOH	1/1	10	438.79±0.36
2	400	NaOH	1/1	10	414.90±0.23
3	100	H_3PO_4	1/1	10	421.99±0.05
4	400	H_3PO_4	1/1	10	410.29±0.03
5	100	NaOH	1/3	10	489.28±0.04
6	400	NaOH	1/3	10	439.36±0.07
7	100	H_3PO_4	1/3	10	443.12±0.01
8	400	H_3PO_4	1/3	10	432.55±0.02
9	100	NaOH	1/1	30	444.64±0.15
10	400	NaOH	1/1	30	424.43±0.09
11	100	H_3PO_4	1/1	30	647,40±0.37
12	400	H_3PO_4	1/1	30	493.74±0.27
13	100	NaOH	1/3	30	524.68±0.09
14	400	NaOH	1/3	30	449.48±0.66
15	**100**	**H_3PO_4**	**1/3**	**30**	**685.35±0.02**
16	400	H_3PO_4	1/3	30	665.55±0.08

Table 2 shows that the iodine index of prepared activated carbons, closely linked to their adsorption capacities, vary according to their preparation conditions. The highest values of 685.35±0.02; 665.55±0.08 and 647.40±0.37 mg/g were obtained for experiments 15, 16 and 11, respectively and the lowest values of 410.29±0.03; 414.90±0.23 and 421.99±0.05 mg/g were obtained for experiments 4, 2 and 3, respectively. These results show the influence of selected factors on AC preparation process as reported in literature (Gueye *et al.*, 2014). The significance test for each coefficient of the model (**Table 3**) was performed considering that a coefficient is statistically

significant if its absolute value is greater than twice the standard deviation (2σ = 19,28) (Assidjo *et al.*, 2005).

Table 3. Model coefficient values

Coefficients	Coefficient values	Absolute value of coefficients	Significant
b_0	489.10	**489.10**	Yes
b_1	-22.81	**22.81**	Yes
b_2	35.90	**35.90**	Yes
b_3	27.07	**27.07**	Yes
b_4	52.81	**52.81**	Yes
b_{12}	-1.66	1.66	No
b_{13}	3.37	3.37	No
b_{14}	-10.80	10.80	No
b_{23}	4.57	4.57	No
b_{24}	45.20	**45.20**	Yes
b_{34}	12.28	12.28	No
Standard deviation (σ) = 19,28		Double standard deviation (2σ) = 19,28	

The analysis of **Table 3** shows that the main coefficients (b_0, b_1, b_2, b_3 and b_4) are all greater than twice the experimental standard deviation value (2 σ =19.28), which means that all four factors X_1, X_2, X_3 and X_4 have a significant influence on the adsorption capacity of prepared activated carbons. In addition, the coefficient of interaction effect between the activating agent and the concentration (b_{24} = 45.20) is also significant on adsorption.

The activating agent can be considered as a very important parameter in production of activated carbons. Indeed, activating agent and its ratio play an important role in the mechanisms of pore creation and their development (Vargas *et al.*, 2012; Telegang Chekem, 2017). In this study, the best activating agent is orthophosphoric acid in a 1/3 impregnation ratio. In addition, increasing its concentration from 10 to 30 % promotes an increase in the iodine index as previously reported in literature for jatropha and peanut shells (Gueye *et al.*, 2014). Thus, equation of response to different factors of the experimental plan is given by the mathematical model (**Eqn. 3**).

$$Y = 489.10 - 22.81X_1 + 35.90X_2 + 27.07X_3 + 52.81X_4 + 45.20X_2X_4 \qquad \textbf{Eqn. 3}$$

The optimal experimental conditions for chemical activation of *Blighia sapida* shells to obtain activated carbon with the best possible adsorption capacity, determined from the iodine index, are those of tests 15. The theoretical optimum obtained with the model (Y_{cal} = 672.89 mg/g) is close to the experimental optimum (Y_{exp} = 685.35 mg/g) with a margin of error of 0.0185 (1.85%).

3.2. Characteristics of activated carbon from *Blighia sapida* shells

3.2.1. Determination of dry matter, humidity and ash contents

Dry matter, moisture and ash contents are recorded in **Table 4**.

Table 4. Dry matter, moisture and ash contents

Dry matter content (%)	Moisture content (%)	Ash content (%)
98.387 ±0.003	1.613 ±0.003	6.56 ±0.06

The results of the analysis show that prepared activated carbon has a high dry matter percentage (98.387 ±0.003 %) as well as low moisture (1.613 ±0.003 %) and ash (6.56 ±0.06 %) contents (**Table 4**). The high dry matter content reflects a high degree of graphitization, a high Superior Calorific Power (SCP) and a high quantity of functional groups (Mamane *et al.*, 2016). A low moisture content indicates a high SCP and the low ash content implies that the biomass is essentially made up of organic matter, and therefore of carbon element (Zhang *et al.*, 2015). So *Blighia sapida* shells could be a good precursor to produce activated carbon.

3.2.2. Elemental composition of activated carbon

The EDS analysis of the AC yielded the results recorded in **Table 5**.

Table 5. Elemental composition of prepared activated carbon

C	O	Na	Al	Fe	Ca	K	H	P
78.35	20.32	0.15	0.00	0.10	0.00	0.00	0.00	1.07

The analysis of **Table 5** reveals that AC obtained has a good carbon content (78.35%) which shows that *Blighia sapida* shells are rich in lignite and indicates good carbonization of the biomass favourable to the production of AC (Danish and Ahmad, 2018). The high relative oxygen content could suggest a strong presence of oxygenated functional groups on the surface of AC.

3.2.3. Chemical characteristic and surface functional groups

Table 6 presents the chemical characteristics and surface functional groups of prepared activated carbon using Boehm method.

Table 6. Chemical characteristics and surface functional groups of prepared activated carbon

Iodine index (mg/g)	Methylene blue index (mg/g)	pHpzc	Total acidity (meq/g)	Total basicity (meq/g)	Character
685.35±0.02	98.7±0,1	4.5±0.2	4,43±0,07	2,68±0,04	Acid

The value of iodine index (685.35±0.02 mg/g) and that of methylene blue index (98.7±0.1 mg/g) could indicate a carbon structure with a microporous tendency (Petrov *et al.*, 2008). However, value of methylene blue index obtained in this study is lower than that of activated carbons from Plantain Spike (Briton *et al.*, 2020), *Hyphaene thebaica* shell and *Tieghmelia* seed (Kiari *et al.*, 2022). This difference could be linked to the concentration of orthophosphoric acid. The pHpzc value of 4.5±0.2, determined from **Figure 2**, shows that prepared activated carbon is acidic. The results of surface functional groups assay showed a total acidity and basicity of 4.43±0.07 meq/g and 2.68±0.04 meq/g, respectively. This indicates that the surface of AC is predominantly acidic, thus reflecting the existence of more oxygenated groups (carboxylic, lactones and phenols) which are very favourable to adsorption (Atheba *et al.*, 2014). The acidic character is also attributed to the nature of chemical impregnation agent (H_3PO_4) as reported in literature (Tchakala *et al.*, 2012). These results agree with pH value at zero charge point (pHpzc = 4.5). However, this AC possesses significant contents of basic functions which would be attributed to the presence of pyrone groups and to ash content (Atheba *et al.*, 2014). The presence of acid and basic sites on the activated carbon suggests that AC prepared could adsorb both anionic and cationic adsorbates (Atheba *et al.*, 2014; Bamba *et al.*, 2009).

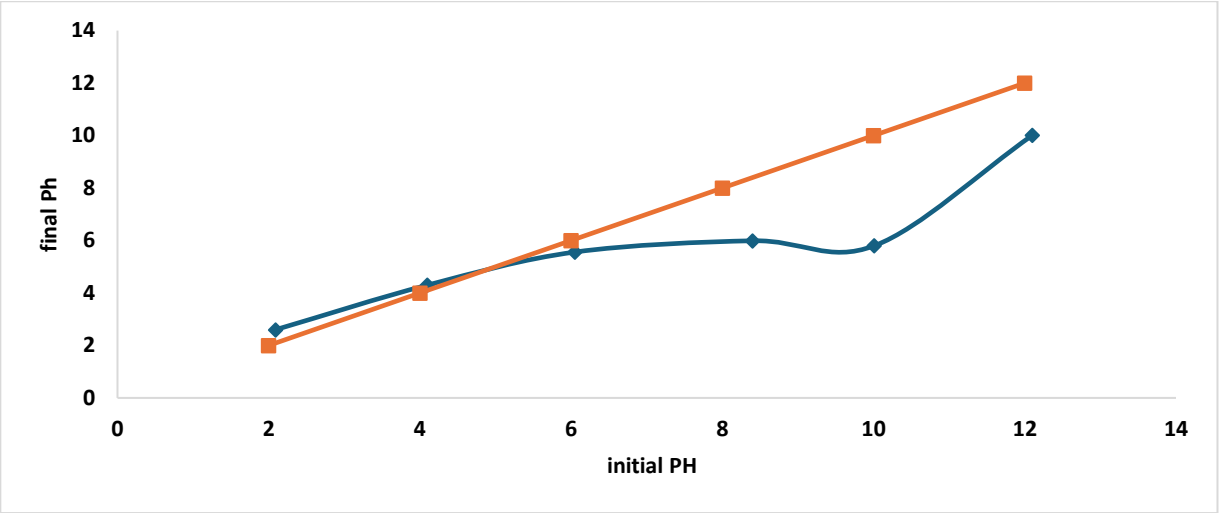

Figure 2. Determination of zero charge pH of activated carbon

3.2.4. Surface morphology, specific surface and porosity

The adsorption-desorption isotherms of nitrogen at 77 K on activated carbon from *Blighia sapida* shells are presented in **Figure 3**.

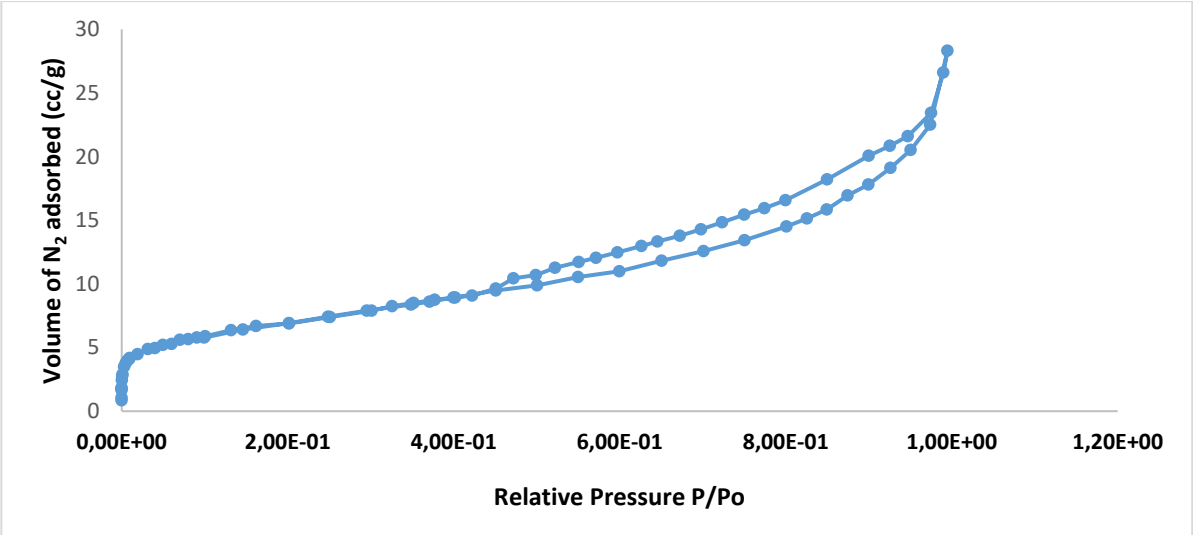

Figure 3. Nitrogen adsorption/desorption isotherm at 77K of activated carbon

The nitrogen adsorption/desorption curve at 77 K indicates a type IV isotherm with a type H_3 hysteresis loop according to the IUPAC classification. This type of isotherm characterizes the simultaneous presence of micropores and mesopores, which suggests that AC prepared is both microporous and mesoporous (Wagn *et al.*, 2020). The porous properties of prepared activated carbon are given in **Table 7**.

Table 7. Porous properties of prepared activated carbon

Total pore volume (cm^3/g)	Mean pore diameter (nm)	Specific surface (m^2/g)
0.905	5.3	681.12

The mean pore diameter obtained by the BJH (Barrett-Joynze-Halenda) method is 5.3 nm, confirming the strong presence of mesopores. The high values of total pore volume (0.905 cm^3/g) and

specific surface (681.12 m^2/g) may explain the presence of mesopores on the walls of prepared activated carbon (Wagn *et al.*, 2020). The external morphology of the activated carbon was visualized by scanning electron microscopy (SEM) and presented in **Figure 4**.

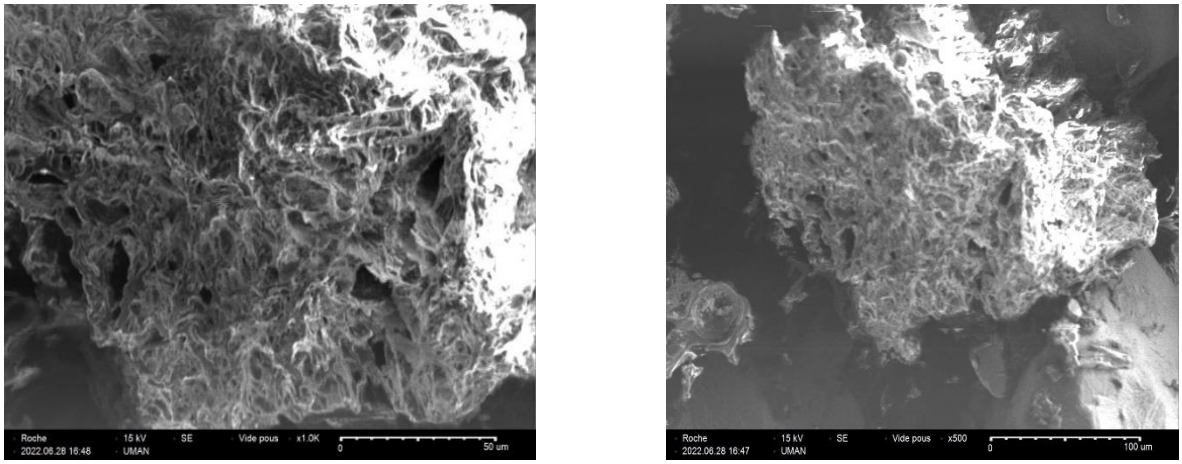

(a) (b)

Figure 4. Morphology of the activated carbon as screen by scanning electron microscope (SEM). Magnification:100 µm (a) and 50 µm (b)

It appears that AC has a rough surface and has many small pores. Similar results were obtained on activated carbons from other agricultural waste (Hamissou *et al.*, 2023; Gouré Bi *et al.*, 2021b; Osobamiro *et al.*, 2020; Kokora *et al.*, 2018).

3.2.5. Surface structure and chemical properties XRD AND IR

The X-ray diffraction (XRD) pattern of activated carbon (**Figure 5**) consists of a very broad line which reflects the absence of structural unity and indicates an amorphous structure and low crystallinity. These results could be due to rapid cooling of the activated carbon at the exit from oven. Furthermore, the peak present at 2θ = 17.38° is characteristic of the allotropic forms of amorphous carbon and graphite (Kan *et al.*, 2017). The Fourier Transform Infra-Red (FTIR) spectrum of the AC is presented in **Figure 6**.

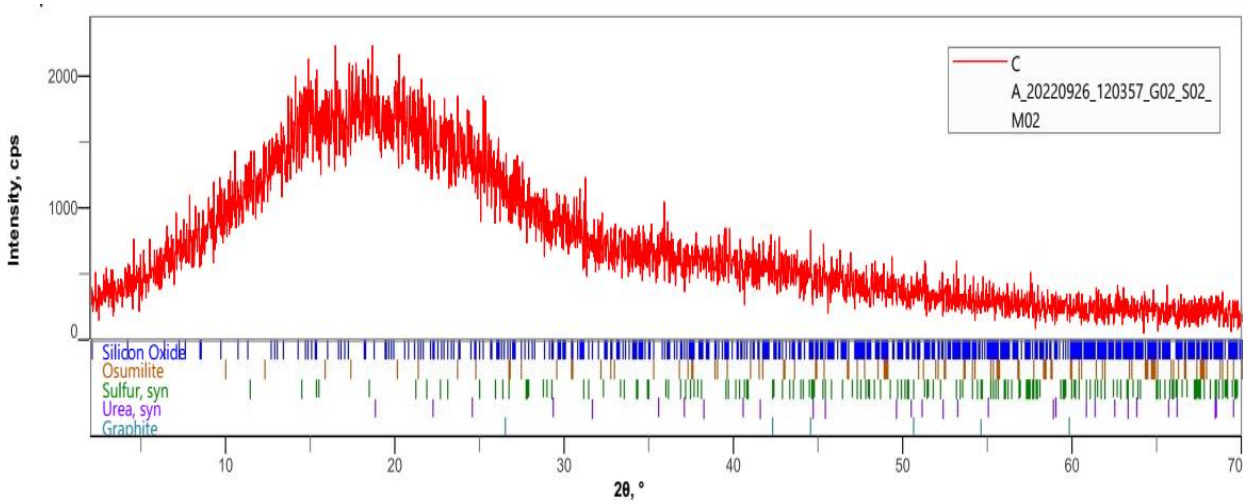

Figure 5. X-ray diffraction diagram of activated carbon

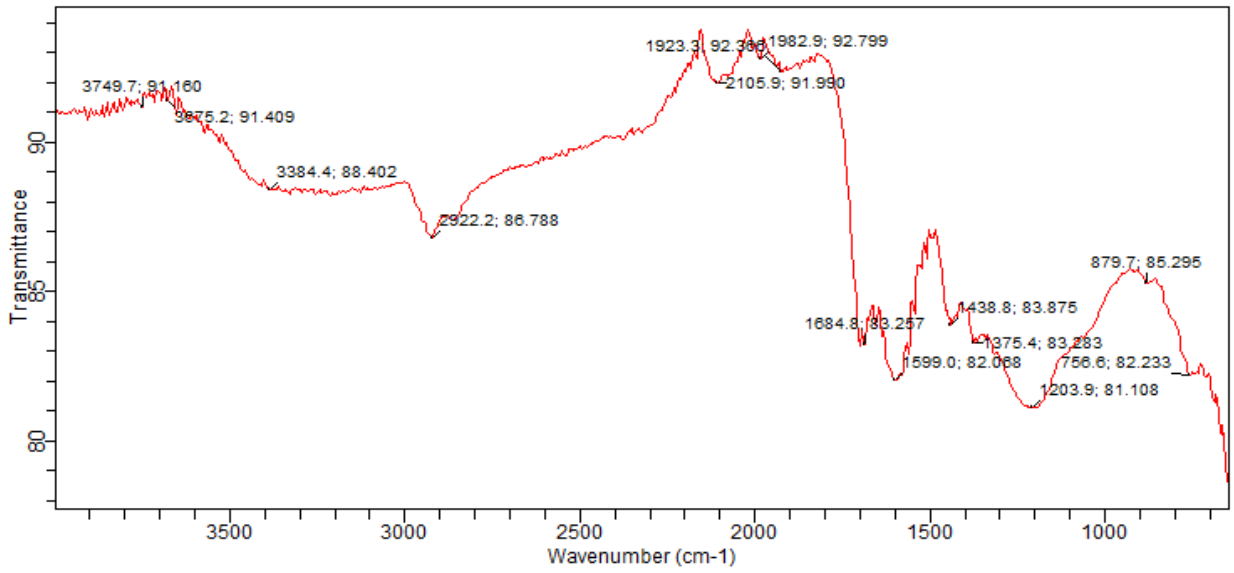

Figure 6. Infrared spectrum of activated carbon

The IR spectrum of AC presents a broad band around 3000 cm^{-1} which could be attributed to the O-H elongation of phenol groups. The broad band, moderately strong at 1600 cm^{-1}, corresponds to the elongation of the C=C bond of benzene groups. The broad band observed between 1800 and 2200 cm^{-1} could correspond to the carbon-oxygen double bonds (C=O) of carboxylic acid or lactone groups. The broad band between 800 and 1000 cm^{-1} could be attributed to the C-O bonds of carboxylic acids (Mastalerz and Bustin, 1996).

Conclusion

An activated carbon was prepared from *Blighia sapida* shells. Modeling of the impregnation and carbonization parameters *via* a complete factorial plan revealed that particle size, activating agent, impregnation ratio and activating agent concentration influence the adsorption capacity of prepared activated carbon. The physical and chemical characterization of prepared carbon shows that the biomass used can produce efficient and good quality activated carbon which could be used for removal of certain pollutants and dye depollution tests are ongoing.

Acknowledgement: The authors are grateful to Mr. Antoine Amani N'GUESSAN, botanist at the laboratory of botany of the department of Agriculture and Animal Resources of the National Polytechnic Institute Félix HOUPHOUET-BOIGNY of Yamoussoukro. His help was invaluable in the authentication of plants.

Disclosure statement: *Conflict of Interest:* The authors declare that there are no conflicts of interest.
Compliance with Ethical Standards: This article does not contain any studies involving human or animal subjects.

References

Adjoumani Y.J., Dablé P.J.M.R., Kouassi K.E., Gueu S., Assémian A.S., Yao K.B. (2019). Modeling and Optimization of Two Clays Acidic Activation for Phosphate Ions Removal in Aqueous Solution by Response Surface Methodology. *J. Water. Resour. Prot.*, 11(02), 200-216. https://doi.org/10.4236/jwarp.2019.112012.

Afrane, G., Achaw, O. (2008). Effect of the concentration of inherent mineral elements on the adsorption capacity of coconut shell-based activated carbons. *Bioresour. Technol.*, 99, 6678–6682. https://doi.org/10.1016/j.biortech.2007.11.071

Assidjo E., Yao B., Akou E., Ado G. (2005). Optimisation of the treatment conditions of cocoa butter in order to reduce non-quality. *J. Chemom.*, 19, 543–548. https://doi.org/10.1002/cem.953

Atheba P., Gbassi G.K., Dongui B., Bamba D., Yolou S., Trokourey A. (2014). Études de la porosité, de la surface spécifique et des fonctions de surface de charbons actifs préparés après carbonisation artisanale des coques de noix de coco. *Les Technologies de Laboratoire* 8 (34), 126-136.

Bamba D., Dongui B., Trokourey A., Zoro G.E., Athéba G.P., Robert D., Wéber J.V. (2009). Etudes comparées des méthodes de préparation du charbon actif, suivies d'un test de dépollution d'une eau contaminée au diuron. *J.Soc.Ouest-Afr*, 028, 41-52.

Basta A.H., Fierro V., Saied H., Celzard A. (2011). Effect of Deashing Rice Straws on Their Derived Activated Carbons Produced by Phosphoric Acid Activation. *Biomass and Bioenergy* 35 (5), 1954-59. https://doi.org/10.1016/j.biombioe.2011.01.043.

Benallou Benzekri M., Benderdouche N., Bestani B., et al. (2018), Valorization of olive stones into a granular activated carbon for the removal of Methylene blue in batch and fixed bed modes, *J. Mater. Environ. Sci.* 9 (1), 272-284. https://doi.org/10.26872/jmes.2018.9.1.31

Brasil J.L., Lucas C.M., Ricardo R.E., Jairton D., Sívio L.P.D., José A., Sales A., Cláudio A., Éder C.L. (2005). Factorial Design for Optimization of Flow-Injection Preconcentration Procedure for Copper(II) Determination in Natural Waters, Using 2-Aminomethylpyridine Grafted Silica Gel as Adsorbent and Spectrophotometric Detection. *IJEAC*, 85 (7), 475-491. https://doi.org/10.1080/03067310500117350.

Briton B.G.H., Yao K.B., Richardson Y., Duclaux L., Reinert L., Soneda Y. (2020). Optimization by Using Response Surface Methodology of the Preparation from Plantain Spike of a Micro-/Mesoporous Activated Carbon Designed for Removal of Dyes in Aqueous Solution. *Arab. J. Sci. Eng.*, 45 (9), 7231-45. https://doi.org/10.1007/s13369-020-04390-0.

Cabal B., Budinova T., Ania C.O., Tsyntsarski B., Parra J.B., Petrova B. (2009). Adsorption of naphthalene from aqueous solution on activated carbons obtained from bean pods. *J. Hazard. Mater.*, 161, 1150–1156.

Crini, G. (2006). Non-conventional low-cost adsorbents for dye removal: A review. Bioresource Technology 97, 1061–1085. https://doi.org/10.1016/j.biortech.2005.05.001

Danish, M., Ahmad, T., 2018. A review on utilization of wood biomass as a sustainable precursor for activated carbon production and application. Renew. Sustain. Energy Rev. 87, 1–21. https://doi.org/10.1016/j.rser.2018.02.003

Eddebbagh M., Abourriche A., Berrada M., Ben Zina M., Bennamara A. (2016). Adsorbent material from pomegranate (Punica granatum) leaves: Optimization on removal of methylene blue using response surface methodology, *J. Mater. Environ. Sci.* 7 (6), 2021-2033.

Fierro V., Muñiz G., Basta A.H., El-Saied H., Celzard A. (2010). Rice Straw as Precursor of Activated Carbons: Activation with Ortho-Phosphoric Acid. *J. Hazard. Mater.* 181 (1-3), 27-34. https://doi.org/10.1016/j.jhazmat.2010.04.062.

Gouré B.I.A., Koné H., Briton B.G.H., Ano J., Soro Y., Yao K. (2021a). Removal of Gentian Violet by Activated Carbon from Mango Kernel Shells (Adams). *Chem. Rev. Lett.* 4, 221-231. https://doi.org/10.22034/crl.2021.306654.1125

Gouré Bi I.A., Briton B.G.H., Soro Y., Ouattara A., Yao K.B. (2021b). Studies of the adsorption parameters of Gentian Violet onto Mango (*Mangifera Indica* Lam) Shell Activated Carbons. *J. Mater. Environ. Sci.*,12 (9), 1226-1242.

Gueye M., Richardson Y., Kafack F.T., Blin J. (2014). High Efficiency Activated Carbons from African Biomass Residues for the Removal of Chromium (VI) from Wastewater. *J. Environ. Chem. Eng.*, 2 (1), 273-81. https://doi.org/10.1016/j.jece.2013.12.014

Hamissou I.G.M., Appiah K.K.E., Konan A.T.S., Sanda M.O., Brou Y.C., et Yao K.B. (2023). Valorization of Cassava Peelings into Biochar: Physical and Chemical Characterizations of Biochar Prepared for Agricultural Purposes. *Scientific African* 20, e01737. https://doi.org/10.1016/j.sciaf.2023.e01737.

Jaramillo J., Gómez-Serrano V., Alvarez P.M. (2009). Enhanced adsorption of metal ions onto functionalized granular activated carbons prepared from cherry stones. *J. Hazard. Mater*, 161, 670–676.

Jodeh S., Basalat N., Abu Obaid A., Bouknana D., Hammouti B., Hada T., Jodeh W. and Warad I. (2014) Adsorption of some organic phenolic compounds using activated carbon from cypress products, *Journal of chemical and pharmaceutical research* 6 (2), 713-723.

Kan Y., Yue Q., Li D., Wu Y., Gao B. (2017). Preparation and Characterization of Activated Carbons from Waste Tea by H_3PO_4 Activation in Different Atmospheres for Oxytetracycline Removal. *J. Taiwan. Inst. Chem. Eng.*,71, 494-500. https://doi.org/10.1016/j.jtice.2016.12.012.

Kiari M.N.A., Fanou G.D., Konan A.T.S., Ouattara A., Kone H., Malam A.M.M., Assidjo N.E., Yao K.B. (2022). Process Conditions Optimization of Plant Waste-Derived Microporous Activated Carbon Using a Full Factorial Design and Genetic Algorithm. *J. Mater. Environ. Sci.* 13 (8), 884-899.

Kokora A.F., Kouadio D.L., Soro D.B., Kossonou N.R., Dembele A. (2018). Elimination d'un colorant de textile sur des adsorbants issus de déchets agricoles. *Rev. Ivoir. Sci. Technol.* 31, 39-54.

Kouadio D.L., Diarra M., Tra Bi T.D., Akesse D.P.V., Soro B.D., Aboua K.N., Meite L., Kone M., Dembele A., Traore K.S. (2019). Adsorption of the Yellow 11 textile dye on activated carbon from the peanut shell. *International Journal of Innovation and Applied Studies*, 26 (4), 1280-1292. DOI: http://www.ijias.issr-journals.org/

Maazou S.D.B., Hima H.I., Malam Alma M.M., Adamou Z., Natatou I. (2018). Elimination du chrome par du charbon actif élaboré et caractérisé à partir de la coque du noyau de *Balanites aegyptiaca*. *Int. J. of Biol. Chem. Sci.* 11 (6), 3050-3065. DOI : https://dx.doi.org/10.4314/ijbcs.v11i6.39

Mamane O.S., Zanguina A., Daou I., Natatou I. (2016). Préparation et caractérisation de charbons actifs à base de coques de noyaux de *Balanites Eagyptiaca* et de *Zizyphus Mauritiana*. *J. Soc. Ouest-Afr. Chim.* 041, 59-67.

Mastalerz M., Bustin R.M. (1996). Application of Reflectance Micro-Fourier Transform Infrared Analysis to the Study of Coal Macerals: An Example from the Late Jurassic to Early Cretaceous Coals of the Mist Mountain Formation, British Columbia, Canada. *Int. J. Coal. Geol.* 32 (1-4), 55-67. https://doi.org/10.1016/S0166-5162(96)00030-4.

Mohammad A., Mohammad A.R., Mohammad A.M., Mohammad B.S. (2007). Adsorption Studies on Activated Carbon Derived from Steam Char. *Indian Society for Surface Science and Technology, India*, 23 (1-2), 73-80.

Muhammad S, Abdul Khalil HPS, Abd Hamid S, Albadn YM, Suriani AB, Kamaruzzaman S, Mohamed A, Allaq AA, Yahya EB. (2022). Insights into Agricultural-Waste-Based Nano-Activated Carbon Fabrication and Modifications for Wastewater Treatment Application. *Agriculture* 12(10), 1737. https://doi.org/10.3390/agriculture12101737

Ndiaye M., Thiam A., Agoyi E.E., Assagbadjo A.E., Dieng B., Noba K. (2023). Valorisation des Espèces Négligées et Sous-Utilisées pour la Sécurité Alimentaire : Traits Morphologiques, Conservation et Regénération des Graines de Blighia sapida K.D. Koenig (Sapindaceae) Suivant les Phytodistricts du Bénin. *European Scientific Journal ESJ*, 19(41), 37. https://doi.org/10.19044/esj.2023.v19n41p37.

Nko'o Abuiboto M.C., Avom J., Mpon R. (2016). Évaluation des propriétés de charbons actifs de résidus de Moabi (Baillonella toxisperma Pierre) par adsorption d'iode en solution aqueuse. *Rev. Sci. L'eau*, 29(1), 51–60. https://doi.org/10.7202/1035716ar

Osobamiro T.M., Adegoke J.A., Osundeko A.O. (2020), Characterization of activated carbon synthesized from Almond and Groundnut shells, *J. Mater. Environ. Sci.*, 11(11), 1903-1913.

Ouattara H., Meite A., Amonkan A.K., Kouame K.G.,Kati-Coulibaly S. (2011). Arille de *Blighia sapida* (K. Koenig, 1778): potentialités nutritionnelles, effets toxiques et carentiels liés à sa consommation, selon le stade de récolte et le degré de consommation. *Int. J. Biol. Chem. Sci.* 5 (1), 392-401. https://doi.org/10.4314/ijbcs.v5i1.68120.

Ouattara L.Y., Kouassi E.K.A., Soro D., Soro Y., Yao K.B., Adouby K., Drogui A.P., Tyagi D.R., Aina P.M. (2021). Cocoa Pod Husks as Potential Sources of Renewable High-Value-Added Products: A Review of Current Valorizations and Future Prospects: A review, BioResources, 16(1), 1988-2020.

Petrov N., Budinova T., Razvigorova M., Parra J., Galiatsatou P. (2008). Conversion of Olive Wastes to Volatiles and Carbon Adsorbents. *Biomass and Bioenergy* 32 (12), 1303-1310. https://doi.org/10.1016/j.biombioe.2008.03.009

Sahu J.N., Agarwal S., Meikap B.C., Biswas M.N. (2009). Performance of a modified multi-stage bubble column reactor for lead(II) and biological oxygen demand removal from waste water using activated rice husk. *J. Hazard. Mater.*, 161, 317–324.

Seung Kim Y., Park C.R. (2016). Titration Method for the Identification of Surface Functional Groups. In *Mater. Sci. Eng. C.*, 273-286. Elsevier. https://doi.org/10.1016/B978-0-12-805256-3.00013-1

Tchakala I., Bawa L.M., Djaneye-Boundjou G., Doni K.S., Nambo P. (2012). Optimisation du procédé de préparation des Charbons Actifs par voie chimique (H_3PO_4) à partir des tourteaux de Karité et des tourteaux de Coton. *Int. J. Biol. Chem. Sci.* 6 (1), 461-78. https://doi.org/10.4314/ijbcs.v6i1.42.

Telegang Chekem C. (2017). Matériaux carbonés multifonctionnels à porosité contrôlée à partir des ressources végétales tropicales : application au traitement de l'eau par photocatalyse. Perpignan : Université de Perpignan, 254 p. Thèse de doctorat : Sciences de l'ingénieur : Université de Perpignan

Vargas D.P., Giraldo L., Moreno-Piraján J.C. (2012). CO_2 Adsorption on Granular and Monolith Carbonaceous Materials. *J. Anal. Appl. Pyrolysis*, 96, 146-52. https://doi.org/10.1016/j.jaap.2012.03.016

Wagn J., Hou G-Y., Wu L.K., Cao H-Z., Zheng G-Q., Tang Y.P. (2020). A Novel Adsorbent of Three-Dimensional Ordered Macro/Mesoporous Carbon for Removal of Malachite Green Dye. *J. Cent. South. Univ.* 27 (2), 388-402. https://doi.org/10.1007/s11771-020-4304-3.

Zhang Z., Feng X., Yue X.X., An F.Q., Zhou W.X., Gao J.F., Hu T.P., Wei C.C. (2015). Effective Adsorption of Phenols Using Nitrogen-Containing Porous Activated Carbon Prepared from Sunflower Plates. *Korean J. Chem. Eng.* 32 (8), 1564-69. https://doi.org/10.1007/s11814-014-0372-0.